arXiv:1704.08439v1 [cond-mat.quant-gas] 27 Apr 2017

Spinor Polariton Condensate: Steady State Phases and Elementary Excitations

Xingran Xu,[1,2,3] Ying Hu,[4,5] Zhidong Zhang,[1,2] and Zhaoxin Liang[3,*]

[1] *Shenyang National Laboratory for Materials Science, Institute of Metal Research, Chinese Academy of Sciences, Shenyang, China*
[2] *School of Materials Science and Engineering, University of Science and Technology of China, Hefei, China*
[3] *Department of Physics, Zhejiang Normal University, Jinhua, 321004, China*
[4] *State Key Laboratory of Quantum Optics and Quantum Optics Devices, Institute of Laser Spectroscopy, Shanxi University, Taiyuan, Shanxi 030006, China*
[5] *Collaborative Innovation Center of Extreme Optics, Shanxi University,Taiyuan, Shanxi 030006, China*

(Dated: April 28, 2017)

Semiconductor microcavity can host spinor polariton condensates with inherent spin multistabilities and fast spin dynamics, promising novel solid-state optoelectronic spin-logic architectures. Here we present a detailed theoretical study on the steady state phases and elementary excitations of a spinor polariton condensate, motivated by recent experimental advances in realizing such systems. We show that a steady homogeneous spinor condensate can exhibit a unpolarized phase and a polarised phase. In each phase, we investigate the elementary excitations using the Bogoliubov de-Gennes approach. We find the spin mode is non-decaying in the unpolarized phase while weakly damped in the polarized phase, along with a gapped energy spectrum which characteristics are indifferent to the reservoir effect. By contrast, the density mode displays rich behavior depending on reservoir parameters. Interestingly, we demonstrate that the 'ghost' branch of the Bogoliubov spectrum of spin mode can be visualized in the photoluminescence emission, distinguishable from that of the density mode and thus allowing for experimental observation, when the spinor polariton condensate is polarized.

PACS numbers: 05.30.Jp, 71.36.+c, 03.75.Kk, 71.35.Lk

At present, there are significant interests and efforts in experimentally realizing the spinor polariton Bose-Einstein condensate (BEC) in semiconductor microcavities[1–3], where exciton-polaritons can emerge from strong couplings between excitons and photons[4–7]. The motivation behind these interests is two-fold. First, recent studies on the one-component polariton BEC[8–18] have revealed a plethora of intriguing phenomena originating from the nonequilibrium nature of the system, where coherent and dissipative dynamics occur on an equal footing[2]. It is of natural interest to explore new phenomena associated with the spin degrees of freedom of polaritons, inherited from the spin properties of their exciton component[19,20], which upon condensation gives rise to a spinor polariton BEC with intrinsic interspecies interaction. Second, owing to the inherent spin multistabilities[21,22] and fast spin dynamics, semiconductor microcavities hosting spinor polariton BECs bring prospects of implementing novel solid-state optoelectronic spin-logic architectures[23,24]. First demonstration of polariton condensates as optical switches in state of the art microcavity structure has been reported in recent experiments[25–33]. It is the purpose of this work to investigate the steady state phases of a spinor polariton BEC, and collective excitations herein, which, despite ongoing experimental efforts[19,20], have not been theoretically addressed so far.

In this work, we are motivated to investigate the mean-field dynamics of a two-component spinor polariton BEC under incoherent pumping. For a steady homogeneous spinor polariton condensate, we identify two phases, i.e., the unpolarized phase and the polarized phase, distinguished by different polarization representing the density difference of the spinor components. We then present a detailed study on the elementary excitations in both phases, mainly the density mode and the spin mode, using the Bogoliubov de-Gennes (BdG) theory.

Our main findings on the properties of the spin modes and density modes of a homogenous spinor polariton condensate are summarized below. The density mode in both phases exhibits different behavior depending on the reservoir parameters: In the fast reservoir limit when reservoir polaritons decay much faster than the condensate, the density excitation features familiar diffusive Goldstone mode at low momenta; instead, a gap opens in the energy spectrum in the opposite slow reservoir limit; In the intermediate regime for the unpolarized phase, we observe an emergence of a maxon-roton-like dispersion in the real part of the excitation spectrum. By contrast, the spin mode is insensitive to the reservoir effects: it is non-decaying in the unpolarized phase while weakly damped in the polarized phase, along with a gapped excitation energy. We find that a homogeneous spinor polariton condensate can be dynamically unstable for attractive interspecies interaction in the slow reservoir limit. We moreover discuss how to probe the presented Bogoliubov dispersions of the spinor polariton condensate. Exploiting the photoluminescence (PL) emission, we show that both the negative energy ghost dispersion branches of the spin mode and density mode can be directly observed in the PL spectrum - well distinguished from each other - when the polariton condensate is in the polarized phase.

The plan of the paper is the following. In Sec. I, we describe the mean field dynamics of a two-component spinor polariton BEC. By solving the stationary state, we identify two phases of the system. In Sec. II, we present a comprehensive study on the elementary excitations using the BdG theory. Analytical solutions in the limiting cases are derived. Then, in Sec. III we discuss how to experimentally probe the presented excitation spectrum exploiting PL emission. We conclude with a summary in Sec. IV.

I. MEAN FIELD DYNAMICS OF A SPINOR POLARITON CONDENSATE

We consider a system of two-component spinor exciton-polariton BEC formed from strong coupling of excitons in a semiconductor quantum well with photons in the microcavity under nonresonant pumping, where spin degrees of freedom are encoded in the left- and right-circular polarizations of polaritons[1–3]. To investigate the mean-field dynamics of the system, we consider a time dependent spinor order parameter $[\psi_1(\mathbf{r},t),\psi_2(\mathbf{r},t)]^T$, the time evolution of which can be effectively described by the dissipative two-component Gross-Pitaevskii equation (GPE)[19,20,34–36], i.e.,

$$i\hbar\frac{\partial\psi_1}{\partial t}=\left[-\frac{\hbar^2\nabla^2}{2m}+g\left|\psi_1\right|^2+g_{12}\left|\psi_2\right|^2+g_R n_R\right]\psi_1 + \Omega\psi_2+\frac{i\hbar}{2}\left(Rn_R-\gamma_C\right)\psi_1, \tag{1}$$

$$i\hbar\frac{\partial\psi_2}{\partial t}=\left[-\frac{\hbar^2\nabla^2}{2m}+g\left|\psi_2\right|^2+g_{12}\left|\psi_1\right|^2+g_R n_R\right]\psi_2 + \Omega\psi_1+\frac{i\hbar}{2}\left(Rn_R-\gamma_C\right)\psi_2. \tag{2}$$

Here, m is the mass of the polariton and g (g_{12}) denotes the interaction strength between polaritons with same (opposite) spins. Note that while polaritons have intrinsic interactions with $g>0$ and $g_{12}<0$, both can be externally tuned by using the bipolariton Feshbach resonance mechanism[37]. The Ω term represents a spin flipping, which arises from the anisotropy-induced splitting of linear polarisations in the microcavity[19], where a coherent transfer of polaritons between the two splitted polarizations exists. Moreover, each component of the spinor polariton condensate is assumed to decay at the same rate γ_C, while coupled to a polariton reservoir of density $n_R(\mathbf{r},t)$ with a coupling strength g_R. We remark that going beyond the Gross-Pitaevskii equations (1) and (2) to fully include the quantum and thermal fluctuations[7] of the quantum field [e.g. Keydlsh path integral method[38–41]] is beyond the scope of this work.

Equations (1) and (2) are assumed to couple to the rate equation for the polariton reservoir as follows, as in Refs.[19,20,34],

$$\frac{\partial n_R}{\partial t}=P-\gamma_R n_R-R\left(\left|\psi_1\right|^2+\left|\psi_2\right|^2\right)n_R. \tag{3}$$

Equation (3) contains an external pumping at a rate P, a decay of reservoir polaritons at rate γ_R, and the spatial hole-burning process due to the scattering of reservoir polaritons into the spinor condensate at a rate R (dubbed the stimulated scattering rate).

Equations (1)-(3) provide complete descriptions on the mean-field dynamics of the spinor polariton BEC coupled to a polariton reservoir, which physics is determined by the interplay among seven parameters: the pump rate P and the relax rate γ_R of the reservoir, the simulated scattering rate R, the loss rate of the condensate polaritons γ_C, the coherent coupling Ω, and the interaction between polaritons g and g_{12}. The steady state for the coupled system and reservoir can be obtained under a continuous-wave and uniform pumping, using an ansatz of the form $\psi_i(\mathbf{r},t)=e^{-i\mu_T t}\psi_i^0$ $(i=1,2)$ and $n_R(\mathbf{r},t)=n_R^0$. As such, a spatially homogeneous spinor polariton BEC as the nonzero steady state solutions of Eqs. (1) - (3) can only exist under the condition $P>P_{\rm th}$ with $P_{\rm th}=\gamma_R\gamma_C/R$, similar as its single-component counterpart. However, depending on the interspecies interaction g_{12}, the spinor polariton BEC can feature two steady-state phases, which are distinguished by the spontaneous spin polarization $\langle S_z\rangle=n_1^0-n_2^0$ acting as the order parameter. Denoting $n_0=\left(P-P_{\rm th}\right)/\gamma_C$ as the total condensate density, we have

- Phase **I**: When $g_{12}<g+2\Omega/n_0$, the spinor polariton BEC is in the *unpolarized* condensate phase characterized by $\langle S_z\rangle=0$. There, the polariton BEC has steady-state solutions $n_1^0=n_2^0=\left(P-P_{\rm th}\right)/(2\gamma_C)$, along with the stationary reservoir density $n_R^0=\gamma_C/R$. The corresponding chemical potential is obtained as $\mu_T=\left(g+g_{12}\right)n_0/2+g_R n_R^0-\Omega$.

- Phase **II**: When $g_{12}>g+2\Omega/n_0$, the spinor polariton BEC is in the *polarized* condensate phase characterized by $\langle S_z\rangle\neq 0$. There, we have $n_1^0-n_2^0=n_0\sqrt{1-[2\Omega/(g-g_{12})n_0]^2}$, while $\mu_T=gn_0+g_R n_R^0$ and $n_R^0=\gamma_C/R$.

At the critical interaction when $g_{12}=g+2\Omega/n_0$, a phase transition in the steady state occurs, which manifests in the divergent behavior of spin-density response function[42]. Consider for example a spin density perturbation to the system Hamiltonian in form of $\lambda\sigma_z e^{(ikx-\omega t)+\eta t}$, with $\eta\to 0^+$. The linear response to this perturbation as represented by the spin density response function is obtained as $\chi_s\propto 1/(g-g_{12}+2\Omega/n_0)$, which diverges at the phase transition. We emphasize that while the spinor polariton condensate possesses a critical condition formally resembling the equilibrium counterpart[43], the open-dissipative nature of our system is implicitly reflected by n_0, controlled by the balance between pumping and decaying.

II. ELEMENTARY EXCITATIONS IN A HOMOGENEOUS SPINOR POLARITON BEC

Equipped with the above knowledge on the steady-state phases of the spinor polariton BEC, next we investigate the corresponding elementary excitations within the Bogoliubov framework[8,44–46]. To this end, we start from the standard decomposition of the wave function $(\psi_1,\psi_2,n_R)^T$ into the steady-state solution $(\psi_1^0,\psi_2^0,n_R^0)^T$ and a small fluctuating term[8,44–46], i.e.,

$$\begin{pmatrix}\psi_1(\mathbf{r},t)\\ \psi_2(\mathbf{r},t)\end{pmatrix}=e^{-i\mu_T t}\begin{pmatrix}\psi_1^0\\ \psi_2^0\end{pmatrix}\left[1+\sum_{\mathbf{k}}\left\{\begin{pmatrix}u_{1\mathbf{k}}\\ u_{2\mathbf{k}}\end{pmatrix}e^{i(\mathbf{kr}-\omega t)}+\begin{pmatrix}v_{1\mathbf{k}}^*\\ v_{2\mathbf{k}}^*\end{pmatrix}e^{-i(\mathbf{kr}-\omega^* t)}\right\}\right], \tag{4}$$

and

$$n_R(\mathbf{r},t)=n_R^0\left[1+\sum_k\left\{w_{\mathbf{k}}e^{i(\mathbf{kr}-\omega t)}+w_{\mathbf{k}}^*e^{-i(\mathbf{kr}-\omega^* t)}\right\}\right]. \tag{5}$$

Substituting Eqs. (4) and (5) into Eqs. (1)-(3) and retaining only first-order terms of fluctuation, we obtain at each momentum $\mathbf{k}$ the Bogoliubov de-Gennes (BdG) equation $\mathcal{L}_{\mathbf{k}}\mathcal{U}_{\mathbf{k}}=\hbar\omega_{\mathbf{k}}\mathcal{U}_{\mathbf{k}}$. Here, $\mathcal{U}_{\mathbf{k}}=(u_{1\mathbf{k}},v_{1\mathbf{k}},u_{2\mathbf{k}},v_{2\mathbf{k}},w_{\mathbf{k}})^T$ and the operator $\mathcal{L}_{\mathbf{k}}$ in the matrix form reads

$$\mathcal{L}_{\mathbf{k}}=\begin{pmatrix} h_1 & gn_1^0 & g_{12}n_2^0-\Omega\sqrt{n_2^0/n_1^0} & g_{12}n_2^0 & g_Rn_R^0+\frac{i}{2}Rn_R^0\\ -gn_1^0 & -h_1 & -g_{12}n_2^0 & -g_{12}n_2^0+\Omega\sqrt{n_2^0/n_1^0} & -g_Rn_R^0+\frac{i}{2}Rn_R^0\\ g_{12}n_1^0-\Omega\sqrt{n_1^0/n_2^0} & g_{12}n_1^0 & h_2 & gn_2^0 & g_Rn_R^0+\frac{i}{2}Rn_R^0\\ -g_{12}n_1^0 & -g_{12}n_1^0+\Omega\sqrt{n_1^0/n_2^0} & -gn_2^0 & -h_2 & -g_Rn_R^0+\frac{i}{2}Rn_R^0\\ -iRn_1^0 & -iRn_1^0 & -iRn_2^0 & -iRn_2^0 & -i\left[Rn_0+\gamma_R\right]\end{pmatrix}, \tag{6}$$

with $h_{1(2)}=\varepsilon_k^0+g_Rn_R^0+2gn_{1(2)}^0+g_{12}n_{2(1)}^0-\mu_T$, where $\varepsilon_k^0=\hbar^2k^2/2m$. Solutions to Eq. (6) provide full specifications of the elementary excitations in the spinor polariton BEC. Note that due to the non-hermitian character of the Liouvillian matrix, Equation (6) will yield five complex dispersion branches: $\omega_j=\Re(\omega_j)+i\Im(\omega_j)$ $(j=1,2,3,4,5)$, where the imaginary part represents the damping spectrum.

Based on Eq. (6), below we present an elaborated study on the Bogoliubov excitation modes of a homogeneous spinor polariton condensate in the unpolarized phase (see Sec. II A) and in the polarized phase (see Sec. II B).

A. Elementary excitations in the unpolarized phase

We first discuss the excitation spectrum in the unpolarized condensate phase, which exists when $g_{12}<g+2\Omega/n_0$. Substituting the corresponding stationary values (see Sec. I) into the BdG Eq. (6), we find

$$\mathcal{L}_{\mathbf{k}}=\begin{pmatrix} h_1 & \frac{gn_0}{2} & \frac{g_{12}n_0}{2}-\Omega & \frac{g_{12}n_0}{2} & g_Rn_R^0+\frac{i}{2}Rn_R^0\\ -\frac{gn_0}{2} & -h_1 & -\frac{g_{12}n_0}{2} & -g_{12}n_2^0+\Omega & -g_Rn_R^0+\frac{i}{2}Rn_R^0\\ \frac{g_{12}n_0}{2}-\Omega & \frac{g_{12}n_0}{2} & h_2 & \frac{gn_0}{2} & g_Rn_R^0+\frac{i}{2}Rn_R^0\\ -\frac{g_{12}n_0}{2} & -\frac{g_{12}n_0}{2}+\Omega & -\frac{gn_0}{2} & -h_2 & -g_Rn_R^0+\frac{i}{2}Rn_R^0\\ -iRn_0/2 & -iRn_0/2 & -iRn_0/2 & -iRn_0/2 & -i\left[Rn_0+\gamma_R\right]\end{pmatrix}, \tag{7}$$

with $h_1=h_2=\varepsilon_k^0+gn_0/2+\Omega$. Before proceeding with the general solutions for Eq. (7), we find it worthwhile to briefly comment on two limiting cases, as presented below. Note that for analytical simplicity, we shall assume $g_R=g$ hereupon.

Two limiting cases - In the limit of vanishing reservoir when $n_R^0\approx 0$ and $R\approx 0$, by disregarding the reservoir effect in Eq. (7) in the leading order we find

$$\mathcal{L}_{\mathbf{k}}=\begin{pmatrix} h_1 & \frac{gn_0}{2} & \frac{g_{12}n_0}{2}-\Omega & \frac{g_{12}n_0}{2}\\ -\frac{gn_0}{2} & -h_1 & -\frac{g_{12}n_0}{2} & -\frac{g_{12}n_0}{2}+\Omega\\ \frac{g_{12}n_0}{2}-\Omega & \frac{g_{12}n_0}{2} & h_2 & \frac{gn_0}{2}\\ -\frac{g_{12}n_0}{2} & -\frac{g_{12}n_0}{2}+\Omega & -\frac{gn_0}{2} & -h_2\end{pmatrix}. \tag{8}$$

In this case the Bogoliubov excitation spectra are found

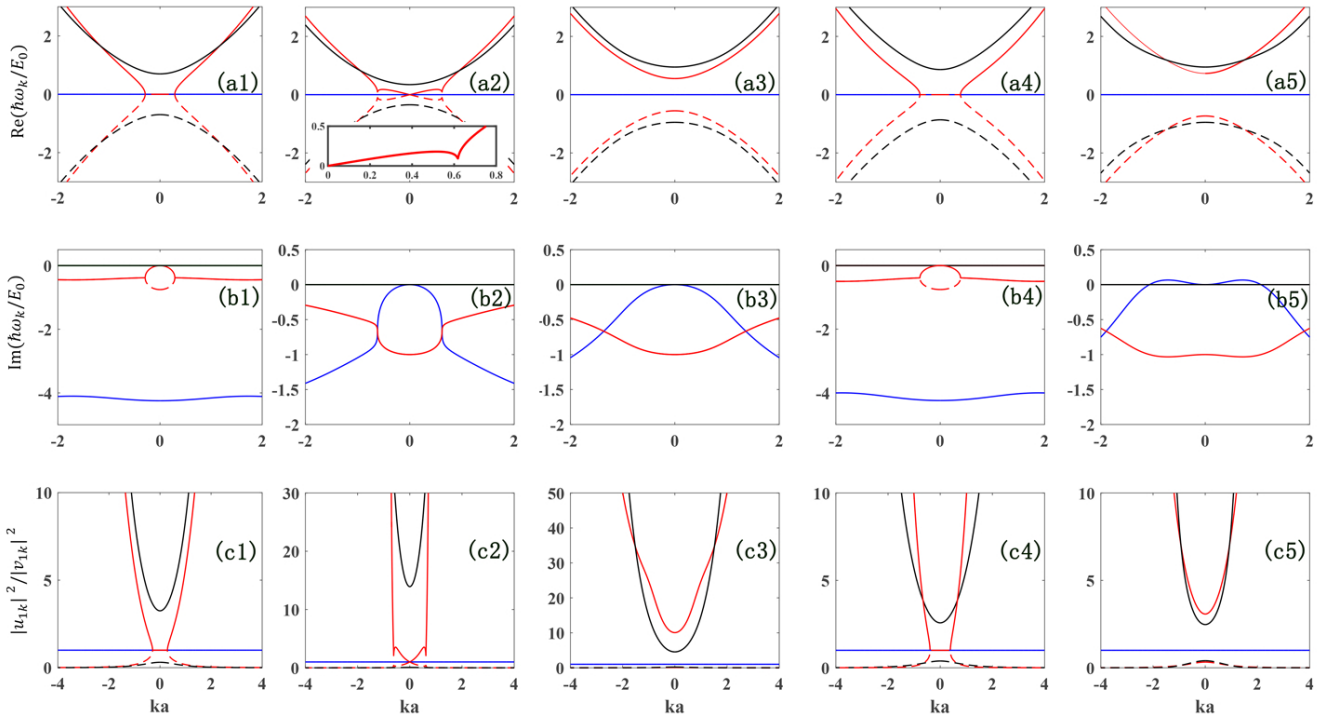

Figure 1. Elementary excitations of a spinor polariton BEC in the unpolarized phase. (a1)-(a5) Real part and (b1)-(b5) imaginary part of the excitation spectra associated with the density modes (red curves), spin modes (black curves) and the reservoir mode (blue curves), respectively; (c1)-(c5) the corresponding Bogoliubov amplitude ratio $|u_{1k}|^2 / |v_{1k}|^2$ for the eigensolutions of the matrix $\mathcal{L}_{\mathbf{k}}$ in Eq. (7). The solid and dashed curves in panels (a1)-(a5) depict the positive and negative energy spectrum of the excitation modes. In all plots, the energy is scaled in units of $E_0 = \hbar^2/2ma^2$ with $a = \sqrt{\hbar^2/mgn_0}$, and we take $\Omega/E_0 = 0.1$. Other parameters [see Eq. (7)] are chosen as follows: (a1)-(c1) $\gamma_R/\gamma_C = 1.8$, $g_{12}/g = 0.3$ and $P/E_0 = 5$; (a2)-(c2) $\gamma_R/\gamma_C = 1$, $g_{12}/g = 0.6$ and $P/E_0 = 2$; (a3)-(c3) $\gamma_R/\gamma_C = 0.1$, $g_{12}/g = 0.3$ and $P/E_0 = 2$; (a4)-(c4) $\gamma_R/\gamma_C = 1.8$, $g_{12}/g = -0.1$ and $P/E_0 = 5$; (a5)-(c5) $\gamma_R/\gamma_C = 0.1$, $g_{12}/g = -0.3$ and $P/E_0 = 2$.

as

$$\hbar\omega_D = \sqrt{\varepsilon_k^0 \left[\varepsilon_k^0 + (g + g_{12})\, n_0\right]}, \tag{9}$$

$$\hbar\omega_S = \sqrt{\varepsilon_k^0 \left(\varepsilon_k^0 + \delta g n_0 + 4\Omega\right) + 2\Omega \left(\delta g n_0 + 2\Omega\right)}, \tag{10}$$

where $\delta g = g - g_{12}$, and ω_D and ω_S correspond to the density mode and the spin-density mode, respectively. Equations (9) and (10) are formally similar as an equilibrium coupled spinor BEC [see e.g., Ref.[43,47]], except of the open-dissipative character reflected by n_0. Particularly, while the density mode is gapless at $k = 0$, the excitation of spin mode has an energy gap $\sqrt{2\Omega\left[\delta g n_0 + 2\Omega\right]}$ due to the coherent transfer (Ω term) of polaritons between the two polarizations, which closing occurs at the critical point when $g_{12} = g + 2\Omega/n_0$. In addition, whereas the density mode behaves as $\omega_D(k) \sim k$ for $k \to 0$, the spin mode has an effective mass: the dispersion near the gap behaves as $\sim k^2$.

In the limit of fast reservoir, when $1/\gamma_R$ is the shortest time scale, an adiabatic elimination of the fast dynamics of reservoir in lowest order of the perturbation theory reduces Eq. (7) to the following matrix form

$$\mathcal{L}_{\mathbf{k}} = \begin{pmatrix} h_1 - \frac{g\Gamma}{2R} - \left(\frac{i}{4}\Gamma + \omega\right) & \frac{gn_0}{2} - \frac{g\Gamma}{2R} - \frac{i}{4}\Gamma & \frac{g_{12}n_0}{2} - \frac{g\Gamma}{2R} - \Omega - \frac{i}{4}\Gamma & \frac{g_{12}n_0}{2} - \frac{g\Gamma}{2R} - \frac{i}{4}\Gamma \\ -\frac{gn_0}{2} + \frac{g\Gamma}{2R} - \frac{i}{4}\Gamma & -h_1 + \frac{g\Gamma}{2R} - \left(\frac{i}{4}\Gamma + \omega\right) & -\frac{g_{12}n_0}{2} + \frac{g\Gamma}{2R} - \frac{i}{4}\Gamma & -g_{12}n_0^2 + \frac{g\Gamma}{2R} + \Omega - \frac{i}{4}\Gamma \\ \frac{g_{12}n_0}{2} - \frac{g\Gamma}{2R} - \Omega - \frac{i}{4}\Gamma & \frac{g_{12}n_0}{2} - \frac{g\Gamma n_0}{2R} - \frac{i}{4}\Gamma & h_2 - \frac{g\Gamma}{2R} - \left(\frac{i}{4}\Gamma + \omega\right) & \frac{gn_0}{2} - \frac{g\Gamma}{2R} - \frac{i}{4}\Gamma \\ -\frac{g_{12}n_0}{2} + \frac{g\Gamma}{2R} - \frac{i}{4}\Gamma & -\frac{g_{12}n_0}{2} + \frac{g\Gamma}{2R} + \Omega - \frac{i}{4}\Gamma & -\frac{gn_0}{2} + \frac{g\Gamma}{2R} - \frac{i}{4}\Gamma & -h_2 + \frac{g\Gamma}{2R} - \left(\frac{i}{4}\Gamma + \omega\right) \end{pmatrix} \tag{11}$$

with $\Gamma = Rn_0\gamma_C / \left(\gamma_R + Rn_0\right)$. The resulting excitation spectra are found as

$$\hbar\omega_D = -\frac{i\Gamma}{2} + \sqrt{\varepsilon_k^0 \left[\varepsilon_k^0 + (g + g_{12})\, n_0\right] - \frac{\Gamma^2}{4}}, \tag{12}$$

$$\hbar\omega_S = \sqrt{\varepsilon_k^0 \left(\varepsilon_k^0 + \delta g n_0 + 4\Omega\right) + 2\Omega \left[\delta g n_0 + 2\Omega\right]}. \tag{13}$$

Comparing Eqs. (10) and (13), we see that the energy $\omega_S(k)$ of the spin mode stays the same in the two limits, contrasting to the density mode whose spectrum is strongly modified by the reservoir [see Eqs. (9) and (12)]. In particular, the low-lying density mode transforms from the sound mode to the characteristic diffusive mode[8], where the real part of the energy is zero while the imaginary part behaves as $\sim k^2$ [see Eq. (12)].

Generic case - For arbitrary parameter γ_R/γ_C, solutions to the BdG Eq. (7) can be exactly cast into the following form

$$\left[(\hbar\omega)^2-(\hbar\omega_S)^2\right]\times\left[(\hbar\omega)^3+i\left(Rn_0+\gamma_R\right)(\hbar\omega)^2-\left[Rn_0\gamma_C+(\hbar\omega_D)^2\right]\hbar\omega+ic(k)\right]=0. \tag{14}$$

Here, ω_S and ω_D are given by Eqs. (9) and (10), and

$$c(k)=-\left(Rn_0+\gamma_R\right)(\hbar\omega_D)^2+gn_0\gamma_C\varepsilon_k^0, \tag{15}$$

which tends to zero for $k\to 0$. Following from Eq. (14), we immediately see that:

(1) There always exists two *real* eigen-solutions $\omega=\pm\omega_S$ representing the real energy of the spin modes, regardless of values of γ_R/γ_C, i.e., the spin modes here are blind to the reservoir and are not damped. Indeed, as confirmed by the numerical results in Fig. 1(a) and (b), the spin modes (black curves) always exhibit a gapped real energy spectrum, and display qualitatively similar features despite variations of γ_R/γ_C. Though, the size of the gap can be tuned via variations of g_{12}/g [c.f. Figs. 1(a1) and (a2)], as expected from Eq. (10).

(2) The spectra of the density modes and the reservoir mode can be obtained from the second bracket in Eq. (14), which, in contrast to the spin mode, display different behavior depending on γ_R/γ_C. In fact, decoupled from the spin mode, the density and reservoir modes are expected to exhibit similar behavior as the one-component polariton condensate[8], except for modifications by the interspecies coupling g_{12} contained in ω_D.

To gain further insight, we solve Eq. (14) for momenta $k=0$ and $k\gg a^{-1}(a=\hbar/\sqrt{mgn_0}$ is the usual coherent length of BEC and we introduce $E_0=\hbar^2/ma^2$), respectively. (i) At $k=0$, we obtain $(\hbar\omega)^3+i\left(Rn_0+\gamma_R\right)(\hbar\omega)^2-Rn_0\gamma_C\hbar\omega=0$, yielding three solutions: $\omega^{(0)}_{k=0}=0$ and

$$\omega^{\pm}_{k=0}=-i\left(\frac{Rn_0+\gamma_R}{2}\right)\pm\sqrt{Rn_0\gamma_C-\frac{1}{4}\left(Rn_0+\gamma_R\right)^2}. \tag{16}$$

Obviously, when $\gamma_C>(Rn_0+\gamma_R)^2/(4Rn_0)$, $\omega^{\pm}_{k=0}$ have finite real components representing an energy gap, i.e. $E_\Delta=(1/2)\sqrt{4Rn_0\gamma_C-\left(Rn_0+\gamma_R\right)^2}$. In this case $\omega^{\pm}_{k=0}$ correspond to gapped density modes decaying at a rate $[Rn_0+\gamma_R]/2$. That is, the density mode becomes massive, as also discussed in Ref.[10] for the one-component polariton BEC taking into account of the effect of the bottleneck polaritons. However, when $\gamma_C\le(Rn_0+\gamma_R)^2/(4Rn_0)$, in particular, when $\gamma_R\gg\gamma_C\sim n_0R$, $\omega^{\pm}_{k=0}$ become purely imaginary with $\omega^{+}_{k=0}\approx -i3\gamma_C^2/(2\gamma_R)$ and $\omega^{-}_{k=0}\approx -i\gamma_R$. While $\omega^{-}_{k=0}$ corresponds to the fast decaying reservoir mode, both $\omega^{+}_{k=0}$ and $\omega^{(0)}_{k=0}$ are associated with the density modes, reflecting the dissipative nature of the diffusive Goldstone mode arising in this regime. (ii) At large momenta $k\gg a^{-1}$, Equation (14) can be approximately solved as: $\omega^{(0)}_{ka\gg1}\sim -i(Rn_0+\gamma_R)$ and $\omega^{\pm}_{ka\gg1}\sim\pm\omega_D-ig_Rn_0\gamma_C\hbar^2\epsilon^0_k/\omega_D^2$, the former corresponding to the reservoir mode while the latter for the density modes. Since the imaginary part of $\omega^{\pm}_{k\to\infty}$ scales as $\sim 1/k^2$ and thus vanishes at $k\to\infty$, we see that the density modes with large momentum behave universally as free particles without being damped, independent of γ_R and γ_C. Moreover, comparing the damping rate of the reservoir modes at $k=0$ and $k\to\infty$, we see that the reservoir modes exhibit similar damping rate when $\gamma_R\gg\gamma_C\sim Rn_0$, as opposed to the case $\gamma_R\ll\gamma_C\sim Rn_0$, where the damping rate of the reservoir mode becomes obviously k-dependent, increasing from 0 (at $k=0$) to a value $\sim Rn_0$ (at $k\to\infty$). Thus, whereas in the fast reservoir limit, the spin mode, the density mode and the reservoir mode almost decouple from each other, in the opposite limit when $\gamma_C>\gamma_R$, the density excitation significantly mixes with the reservoir, in particular, the system dynamics at large times $t\gg\gamma_C^{-1}$ is strongly influenced by the slowly-decaying low-momentum reservoir modes.

Above analysis are corroborated by the numerical results of excitation spectra for various parameters, as summerized in Fig. 1. For the density modes (see red curves), we observe the characteristic Goldstone branch when $\gamma_R\gg\gamma_C$ [see Figs. 1(a1) and (a4)], which however disappears if $\gamma_R\ll\gamma_C$ when an energy gap appears instead [see Fig. 1(a3) and (a5)]. Physically, the existence of the Goldstone mode in presence of a fast decaying reservoir can also be understood from the following perspective: when $\gamma_R\gg\gamma_C$, the (fast) reservoir is able to adiabatically follow the slow rotation of the condensate phase across the sample, i.e., adiabatically follow the Goldstone mode. At large momenta, we see that the density modes exhibit $\mathrm{Re}(\omega_k)\sim k^2$ and a suppressed damping for all parameters, as discussed earlier. Interestingly, in the crossover regime $\gamma_R\sim\gamma_C$ where the reservoir effect strongly influence the spectrum of the density mode, we observe emergence of a dispersion (real part) that pos-

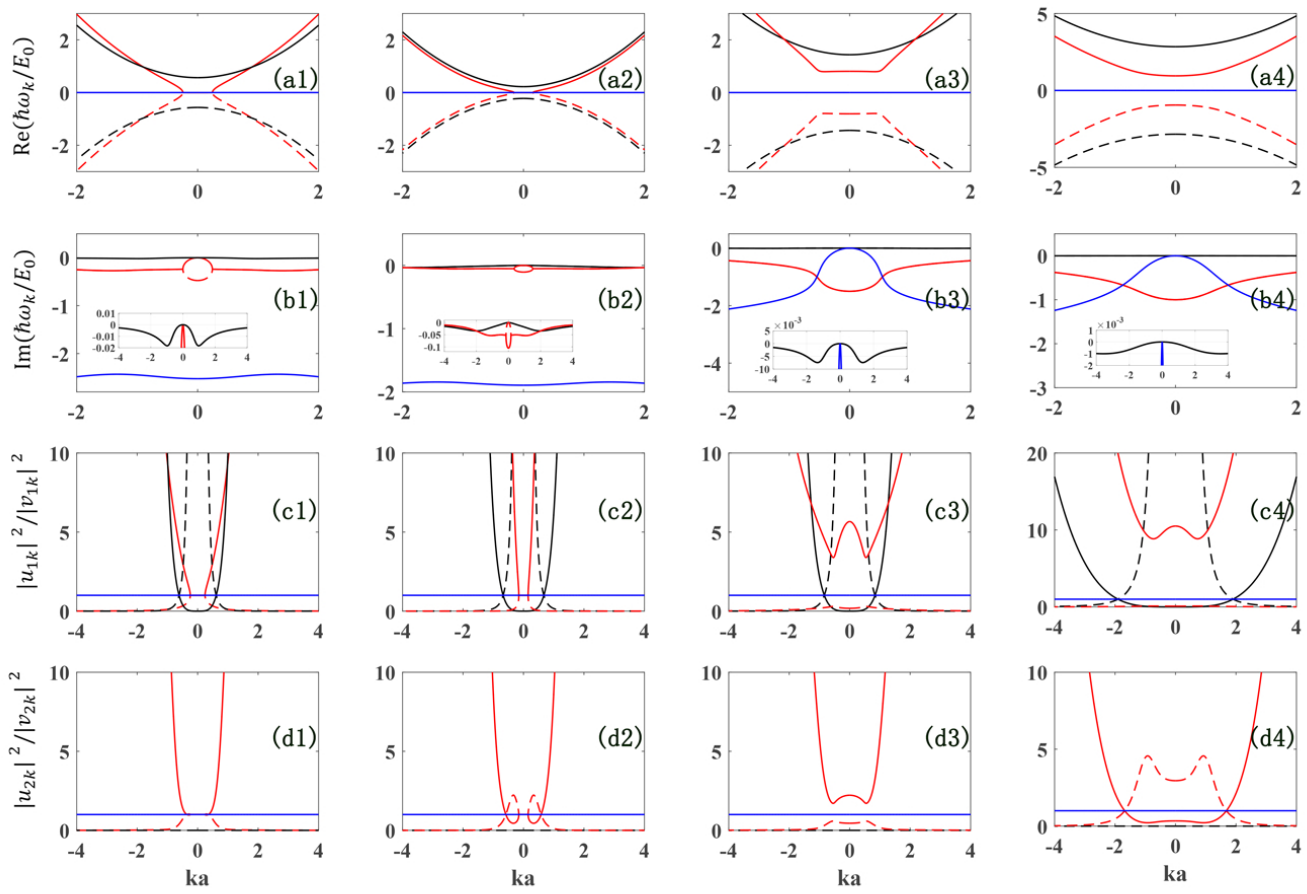

Figure 2. Elementary excitations for spinor polariton BEC in the polarized phase. (a1)-(a4) Real part and (b1)-(b4) imaginary part of the excitation spectra associated with the density modes (red curves), spin modes (black curves) and reservoir modes (blue curves); ratios of Bogoliubov amplitudes (c1)-(c4) $|u_{1\mathbf{k}}|^2/|v_{1\mathbf{k}}|^2$ and (d1)-(d4) $|u_{2\mathbf{k}}|^2/|v_{2\mathbf{k}}|^2$ for eigen-solutions of the matrix $\mathcal{L}_{\mathbf{k}}$ in Eq. (6). For parameters in Eq. (6), we take (a1)-(d1) $\gamma_R/\gamma_C = 1.8$, $g_{12}/g = 1.5$, $P/E_0 = 3$ and $R/E_0 = 1$; (a2)-(d2) $\gamma_R/\gamma_C = 1.8$, $g_{12}/g = 2.5$ and $P/E_0 = 2$; (a3)-(d3) $\gamma_R/\gamma_C = 0.1$, $g_{12}/g = 1.5$ and $P/E_0 = 3$; (a4)-(d4) $\gamma_R/\gamma_C = 0.1$, $g_{12}/g = 2.5$ and $P/E_0 = 2$. In all plots, the energy is scaled in unit of $E_0 = \hbar^2/2ma^2$ with $a = \sqrt{\hbar^2/mgn_0}$ and we have taken $\Omega/E_0 = 0.1$.

sesses a *maxon-roton-like* character [see Fig. 1(a2)], i.e., a softening of an excitation mode occurs at intermediate momentum.

Furthermore, in the regime $\gamma_R \ll \gamma_C \sim Rn_0$, for $g_{12} < 0$ corresponding to attractive interspecies interaction, a spatially homogeneous spinor polariton condensate becomes dynamically unstable, due to an exponential grow of reservoir modulations with time: the reservoir mode shows $\mathrm{Im}[\omega_k] > 0$ at small momenta [see black curves in Fig. 1(b5)]. Instead, such dynamical instability disappears if $g_{12} > 0$ is taken instead [see Fig. 1(b3)]. To understand this, we seek the condition for a homogeneous spinor condensate to be stable in the considered regime by solving Eq. (14) at small momenta. Recall that in this case, the reservoir mode has $\omega = 0$ at $k = 0$, therefore, we expect $\omega(k)$ to be small at $k \to 0$. Retaining only the term linear in ω in Eq. (14), we find $\hbar\omega_{k\to 0} \approx ic(k)/(Rn_0\gamma_C + \omega_D^2)$, with $c(k)/E_0^2 \approx -2(ka)^2[(1 + g_{12}/g)(Rn_0 + \gamma_R) - \gamma_C]$. Thus in order for the low-lying reservoir mode to be stable requires $c(k) \leq 0$, giving the stability condition

$$\left(\frac{g + g_{12}}{g}\right)\frac{Rn_0 + \gamma_R}{\gamma_c} > 1.$$

Obviously, for the parameter regime $Rn_0 \sim \gamma_C \gg \gamma_R$, the above criterion sustains for $g_{12} > 0$ but is violated when $g_{12} < 0$, explaining what we see in Fig. 1(b5). For $g_{12} < 0$, $c(k)$ can change its sign from positive to negative when the momentum increases to values larger than $k_R \neq 0$, where k_R is determined by $c(k_R) = 0$ giving $k_R a \approx \sqrt{2[\gamma_C/(Rn_0 + \gamma_R) - (g + g_{12})/g]}$, i.e., the stability condition is violated at momenta $0 < k < k_R$ [see

Fig. 1(b5)], leading to growing perturbations.

To better understand the behavior of the density mode and the spin-density mode in the unpolarized phase of the spinor polariton BEC, we illustrate the corresponding eigenvectors in Fig. 1(c). There, we plot $u_{1\mathbf{k}}/v_{1\mathbf{k}}$ as a function of k, having in mind that in a unpolarized polariton condensate the density mode (in-phase) features $u_{1\mathbf{k}} = u_{2\mathbf{k}}$ and $v_{1\mathbf{k}} = v_{2\mathbf{k}}$ while the spin mode (out-of-phase) is characterized by $u_{1\mathbf{k}} = -u_{2\mathbf{k}}$ and $v_{1\mathbf{k}} = -v_{2\mathbf{k}}$. These equalities no longer apply for the polarized phase discussed later in Sec. II B. As shown, for $\gamma_R/\gamma_C \geq 1$ [Figs. 1(c1), (c2) and (c4)], the eigenvectors of the Goldstone mode show the usual infrared divergence $v_{1\mathbf{k}} \to k^{-1/2}$ and $u_{1\mathbf{k}} \to -v_{1\mathbf{k}}$ at $k \to 0$, giving rise to $|u_{1\mathbf{k}}/v_{1\mathbf{k}}| = 1$ at $k = 0$. By contrast, for $\gamma_R/\gamma_C \ll 1$ when the density modes exhibit an energy gap, we see that $|u_{1\mathbf{k}}/v_{1\mathbf{k}}| > 1$ for momenta $k \to 0$ [see red curves in Figs. 1(c3) and (c5)], which behavior is also observed in the plot of $|u_{2\mathbf{k}}/v_{2\mathbf{k}}|$ for the gapped spin mode at small momenta [see black curves in Fig. 1(c)].

B. Elementary excitations in the polarized phase

We now turn to the elementary excitations in the polarized phase in the parameter regime $g_{12} > g + 2\Omega/n_0$, which is characterized by unbalanced population $n_1^0 - n_2^0 \neq 0$ [see Sec. I]. The BdG Eq. (6) now takes the form

$$\mathcal{L}_{\mathbf{k}} = \begin{pmatrix} h_1 & \frac{gn_0(1+\Delta)}{2} & \frac{g_{12}n_0(1-\Delta)}{2} - \Omega\sqrt{\frac{1-\Delta}{1+\Delta}} & \frac{g_{12}n_0(1-\Delta)}{2} & g_R n_R^0 + \frac{i}{2}Rn_R^0 \\ -\frac{gn_0(1+\Delta)}{2} & -h_1 & -\frac{g_{12}n_0(1-\Delta)}{2} & -\frac{g_{12}n_0(1-\Delta)}{2} + \Omega\sqrt{\frac{1-\Delta}{1+\Delta}} & -g_R n_R^0 + \frac{i}{2}Rn_R^0 \\ \frac{g_{12}n_0(1-\Delta)}{2} - \Omega\sqrt{\frac{1-\Delta}{1+\Delta}} & \frac{g_{12}n_0(1-\Delta)}{2} & h_2 & \frac{gn_0(1-\Delta)}{2} & g_R n_R^0 + \frac{i}{2}Rn_R^0 \\ -\frac{g_{12}n_0(1-\Delta)}{2} & -\frac{g_{12}n_0(1-\Delta)}{2} + \Omega\sqrt{\frac{1-\Delta}{1+\Delta}} & -\frac{gn_0(1-\Delta)}{2} & -h_2 & -g_R n_R^0 + \frac{i}{2}Rn_R^0 \\ -i\frac{n_0}{2}(1+\Delta)R & -i\frac{n_0}{2}(1+\Delta)R & -i\frac{n_0}{2}(1-\Delta)R & -i\frac{n_0}{2}(1-\Delta)R & -i[Rn_0 + \gamma_R] \end{pmatrix}, \tag{17}$$

with $\Delta = \sqrt{1 - [2\Omega/(g - g_{12})n_0]^2}$, $h_1 = \varepsilon_k^0 + gn_0\Delta + g_{12}n_0(1-\Delta)/2$ and $h_2 = \varepsilon_k^0 - gn_0\Delta + g_{12}n_0(1+\Delta)/2$. In the limit of vanishing reservoir, Eq. (17) reduces to

$$\mathcal{L}_{\mathbf{k}} = \begin{pmatrix} h_1 & \frac{gn_0(1+\Delta)}{2} & \frac{g_{12}n_0(1-\Delta)}{2} - \Omega\sqrt{\frac{1-\Delta}{1+\Delta}} & \frac{g_{12}n_0(1-\Delta)}{2} \\ -\frac{gn_0(1+\Delta)}{2} & -h_1 & -\frac{g_{12}n_0(1-\Delta)}{2} & -\frac{g_{12}n_0(1-\Delta)}{2} + \Omega\sqrt{\frac{1-\Delta}{1+\Delta}} \\ \frac{g_{12}n_0(1-\Delta)}{2} - \Omega\sqrt{\frac{1-\Delta}{1+\Delta}} & \frac{g_{12}n_0(1-\Delta)}{2} & h_2 & \frac{gn_0(1-\Delta)}{2} \\ -\frac{g_{12}n_0(1-\Delta)}{2} & -\frac{g_{12}n_0(1-\Delta)}{2} + \Omega\sqrt{\frac{1-\Delta}{1+\Delta}} & -\frac{gn_0(1-\Delta)}{2} & -h_2 \end{pmatrix}. \tag{18}$$

Solutions of the eigen-energies are found as:

$$\begin{aligned} \left(\hbar\omega_{S/D}\right)^2 &= \varepsilon_k^0\left(\varepsilon_k^0 + g_{12}n_0\right) + \frac{1}{2}\beta - 2\Omega^2 \\ &\pm \sqrt{\left[(\varepsilon_k^0(g_{12} - 2g)n_0 + \frac{1}{2}\beta\right]^2 + \Omega^2\left[\frac{\hbar^4k^4(3g - g_{12})}{m\,(g_{12} - g)} + 2\frac{\hbar^2k^2}{m}n_0(2g - g_{12}) - 2\beta\right] + 4\Omega^4}, \end{aligned} \tag{19}$$

where $\beta = (g - g_{12})^2 n_0^2$ and, as before, $\hbar\omega_S$ and $\hbar\omega_D$ represent energies of the spin mode and the density mode, respectively. As in the unpolarized phase, the density mode is gapless while the spin mode has an energy gap $\omega_S(k) \to \sqrt{(g - g_{12})^2 n_0^2 - 4\Omega^2}$.

In presence of a fast decaying reservoir when $\gamma_R/\gamma_C \gg 1$, Equation (17) at the lowest order of $1/\gamma_R$ reads

$$\mathcal{L}_{\mathbf{k}}=\begin{pmatrix} h_1 & \tilde{g}n_1^0 & \tilde{g}_{12}n_2^0-\Omega\sqrt{\frac{n_2^0}{n_1^0}} & \tilde{g}_{12}n_2^0 \\ -\tilde{g}^*n_1^0 & -h_1^* & -\tilde{g}_{12}^*n_2^0 & -\tilde{g}_{12}^*n_2^0+\Omega\sqrt{\frac{n_2^0}{n_1^0}} \\ \tilde{g}_{12}n_1^0-\Omega\sqrt{\frac{n_1^0}{n_2^0}} & \tilde{g}_{12}n_1^0 & h_2 & \tilde{g}n_2^0 \\ -\tilde{g}_{12}^*n_1^0 & -\tilde{g}_{12}^*n_1^0+\Omega\sqrt{\frac{n_1^0}{n_2^0}} & -\tilde{g}^*n_2^0 & -h_2^* \end{pmatrix},$$

with $\tilde{g}=g-\gamma(g+\frac{i}{2}R)$, $\tilde{g}_{12}=g_{12}-\gamma(g+\frac{i}{2}R)$, $\gamma=\gamma_C/(n_0R+\gamma_R)$, $h_1=\varepsilon_k^0+g_{12}n_2^0+\left[g-\gamma(g+\frac{i}{2}R)\right]n_1^0-gn_2^0$, and $h_2=\varepsilon_k^0+g_{12}n_1^0+\left[g-\gamma\left(g+\frac{i}{2}R\right)\right]n_2^0-gn_1^0$. The eigen-energy is solution to the following equation

$$\left[(\hbar\omega)^2-a^2\right]\times\left[(\hbar\omega-ib)^2-c^2\right]+d=0, \tag{20}$$

with

$$\begin{aligned} b&=-\frac{1}{2}n_0R\gamma, \\ a^2&=\left[\varepsilon_k^0+(g_{12}-g)n_0\right]\left[\varepsilon_k^0+(g_{12}-g)\left(n_1^0-n_2^0\right)\right], \\ c^2&=-gn_0\varepsilon_k^0\gamma+(\varepsilon_k^0)^2-\frac{1}{4}n_0^2R^2\gamma^2+\varepsilon_k^0(g_{12}-g)\left(n_1^0-n_2^0\right)+\varepsilon_k^0n_0(g+g_{12}), \\ d&=-4\varepsilon_k^0\Omega^2\left[n_0(g_{12}-g)+\varepsilon_k^0\right]\frac{n_1^0-n_2^0}{n_0}. \end{aligned}$$

To gain insight into Eq. (20), consider $k=0$ where Eq. (20) allows easy solutions: (i) solutions $\omega_s=\pm\sqrt{(g_{12}-g)^2n_0^2-4\Omega^2}$ correspond to the energy gap of the spin-density modes, (ii) solutions $\omega_D^{(1)}=0$ and $\omega_D^{(2)}=-in_0R\Gamma/2$ are associated with the density modes at $k=0$, near which the imaginary part scales as $\sim k^2$, indicating the existence of diffusive Goldstone mode. Noticing that the energy gap of the spin mode is formally the same as the equilibrium counterpart [see Eq. (19) at $k=0$], we anticipate the behavior of the spin mode is qualitatively unaffected by the the incoherent polariton reservoir, as in the unpolarized condensate. In fact, one can show that for arbitrary value of γ_R/γ_C, the BdG Eq. (17) yields the following equation:

$$\left[(\hbar\omega)^2-(\hbar\omega_D)^2\right]\left[(\hbar\omega)^2-(\hbar\omega_S)^2\right]\left[i\left(Rn_0+\gamma_R\right)+\hbar\omega\right]+i\left(n_0\gamma_C\right)\left(g\frac{\hbar^2k^2}{m}+iR\left(\hbar\omega\right)\right)\left[(\hbar\omega)^2+F(k)\right]=0, \tag{21}$$

Here, $F(k)=4\Omega^2-\left[n_0(g_{12}-g)+\epsilon_k^0\right]^2+2\Omega^2k^2/(g_{12}-g)$, and $\omega_{S/D}$ are defined in Eq. (19). At $k=0$, Eq. (21) admits solutions: $\omega=0$, $\omega=-i(Rn_0+\gamma_R)/2\pm\sqrt{Rn_0\gamma_C-(Rn_0+\gamma_R)^2/4}$ and $\omega=\pm\omega_S$ (evaluated at $k=0$). Indeed, we see that the energy gap of the spin modes stays the same without modification from the polariton reservoir. Meantime, we see that a diffusive Goldstone mode exists as long as $\gamma_C\leq(Rn_0+\gamma_R)^2/(4Rn_0)$ holds, whereas an energy gap opens in the spectrum of the density excitation for $\gamma_C>(Rn_0+\gamma_R)^2/(4Rn_0)$.

In Fig. 2 (a) and (b), we illustrate the excitation spectra for various parameters. We see that, different from the unpolarized phase, the spin modes excited in the polarized phase show a very weak damping [see black curves in Fig. 2 (b) and insets], along with a gapped (real part) energy spectrum. In addition, the density modes and the reservoir modes exhibit similar features as their correspondence in the unpolarized phase. In Figs. 2 (c) and (d), we plot both $|u_{1\mathbf{k}}/v_{1\mathbf{k}}|$ and $|u_{2\mathbf{k}}/v_{2\mathbf{k}}|$ as functions of k. Again, when $\gamma_R/\gamma_C\gg1$, we see that the presence of a diffusive Goldstone mode gives rise to $|u_{1\mathbf{k}}/v_{1\mathbf{k}}|\to1$ (or $|u_{2\mathbf{k}}/v_{2\mathbf{k}}|\to1$) for $k\to0$ [see red curves in Figs. 2(d1), and (d2)]. By contrast, when $\gamma_R/\gamma_C\ll1$ where both the density modes and spin-density modes are gapped, we have $|u_{1\mathbf{k}}/v_{1\mathbf{k}}|>1$ ($|u_{2\mathbf{k}}/v_{2\mathbf{k}}|>1$) at small momenta [see Figs. 2(c3), (c4), (d3), and (d4)].

III. PHOTOLUMINESCENCE OF A SPINOR POLARITON CONDENSATE

In this section, we discuss how to experimentally probe the various Bogoliubov dispersions of a spinor polariton condensate presented in this work. Recently, significant experimental progress have been achieved on measuring

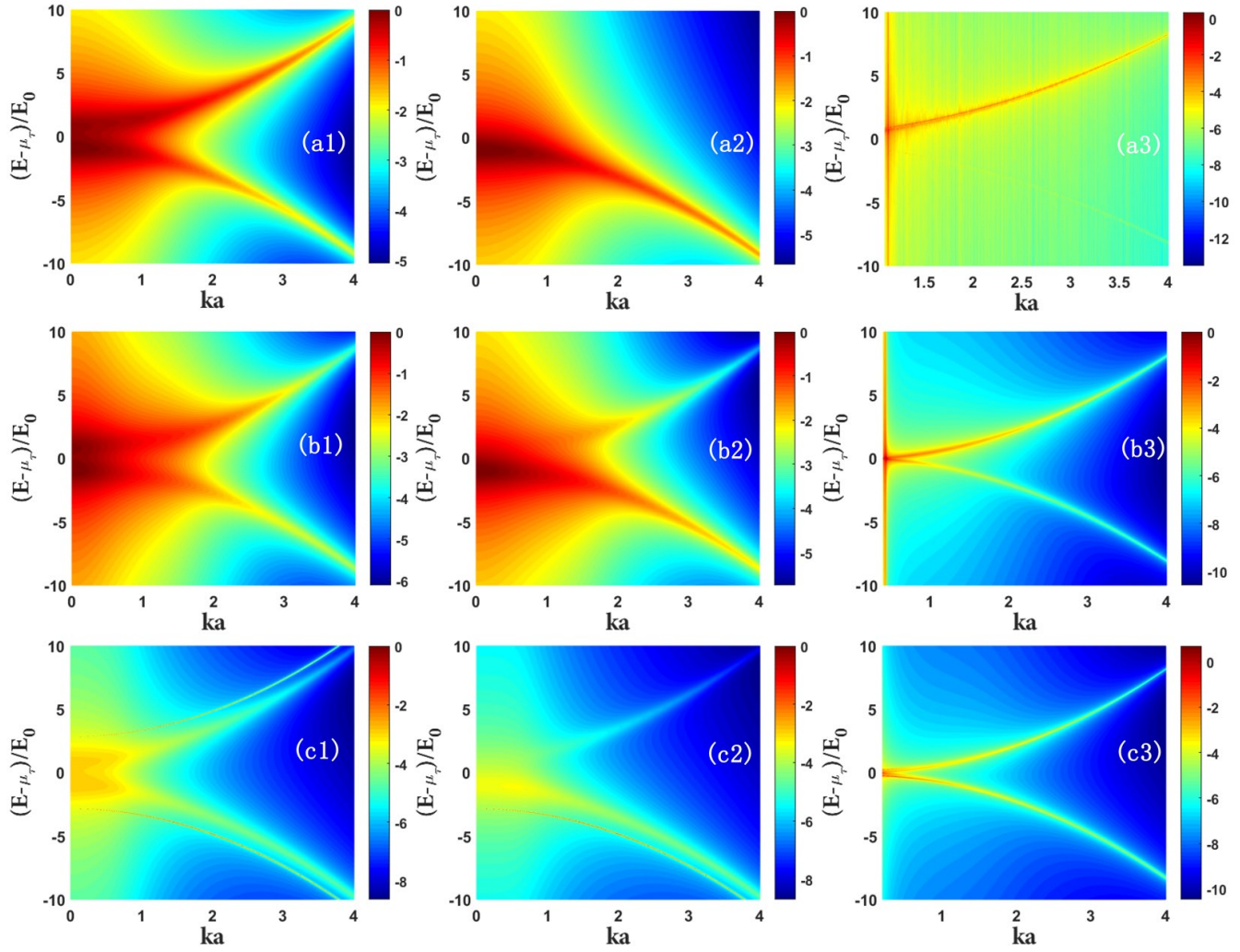

Figure 3. (Color online) PL spectrum $\log_{10}(PL/PL_{max})$ [see Eq. (23)] of a spinor polariton condensate for different parameters. Panels (a)-(b): PL spectrum of a unpolarized spinor polariton condensate with (a) $g_{12} > 0$ and (b) $g_{12} < 0$. Panel (c): PL spectrum of a polarized spinor polariton condensate. For other parameters, we take (a1) $g_{12}/g = 0.3$, $\gamma_R/\gamma_C = 0.1$ and $k_BT/E_0 = 2$; (a2) $g_{12}/g = 0.3$, $\gamma_R/\gamma_C = 0.1$ and $k_BT/E_0 = 0.1$; (a3) $g_{12}/g = 0.3$, $\gamma_R/\gamma_C = 1.8$ and $k_bT/E_0 = 2$; (b1) $g_{12}/g = -0.3$, $\gamma_R/\gamma_C = 0.1$ and $k_BT/E_0 = 2$; (b2) $g_{12}/g = -0.3$, $\gamma_R/\gamma_C = 0.1$ and $k_BT/E_0 = 0.1$; (b3) $g_{12}/g = -0.3$, $\gamma_R/\gamma_C = 1.8$ and $k_bT/E_0 = 0.1$; (c1) $g_{12}/g = 2.5$, $\gamma_R/\gamma_C = 0.1$ and $k_BT/E_0 = 2$; (c2) $g_{12}/g = 2.5$, $\gamma_R/\gamma_C = 0.1$ and $k_BT/E_0 = 0.1$; (c3) $g_{12}/g = 2.5$, $\gamma_R/\gamma_C = 1.8$ and $k_BT/E_0 = 0.1$. In all plots, the energy is in unit of E_0, and $\Omega/E_0 = 0.1$.

elementary excitations of a one-component polariton condensate, aiming particularly at observing two features: (1) The diffusive Goldstone modes, which find origin in the driven-dissipative character of the system[8,9]; (2) The negative energy ghost branch (GB) of the Bogoliubov dispersion, which arises from the hole component of excitations and thus mirror images the normal positive energy branch (NB). In experiments reported in Ref.[48,49], while NB has been directly observed in the photoluminescence (PL) of a nonresonant polariton condensate[50,51], no fingerprints of GB were spotted. Since the GB signal may be easily masked by strong emission, whether it is possible to detect GB in a non-resonant polariton BEC was subjected to debate. On the other hand, the GB dispersion was detected in a resonantly pumped polariton condensate using the four-wave mixing technique, as reported in Ref.[52]. Remarkably, the first successful observation of the PL signal reflecting GB in a non-resonant polariton condensate was reported in Ref.[53]. Motivated by these experimental advances, below we are interested in studying the PL spectra of a spinor polariton BEC under non-resonant pumping, in particular the visibility herein of the ghost branches of dispersions of both the density mode and spin mode, extending relevant work on one-component polariton BECs[10,54].

At the heart of the measurement of the excitation spectrum with PL is the measurement of two-time correlation function of the spinor polariton condensate. Denoting the PL spectrum by $\mathrm{PL}(k,\omega)$, we exploit the approach in Ref.[10,27] and calculate as follows. Defining a matrix

V^{-1} in the form

$$V^{-1}=\begin{pmatrix} \overline{u}_{11} & \overline{u}_{12} & \overline{u}_{13} & \overline{u}_{14} & \overline{u}_{15} \\ \overline{u}_{21} & \overline{u}_{22} & \overline{u}_{23} & \overline{u}_{24} & \overline{u}_{25} \\ \overline{u}_{31} & \overline{u}_{32} & \overline{u}_{33} & \overline{u}_{34} & \overline{u}_{35} \\ \overline{u}_{41} & \overline{u}_{42} & \overline{u}_{43} & \overline{u}_{44} & \overline{u}_{45} \\ \overline{u}_{51} & \overline{u}_{52} & \overline{u}_{53} & \overline{u}_{54} & \overline{u}_{55} \end{pmatrix}, \tag{22}$$

we diagonalize the Bogoliubov's matrix [see Eq. (6)] as $V^{-1}\mathcal{L}_{\mathbf{k}}V=(E_1,-E_1^*,E_1,-E_2^*,E_3)$. Here, the eigenvalues E_1, E_2, and E_3 correspond to the density mode, spin-density mode and reservoir mode, respectively. The PL spectrum can then be derived as

$$\begin{aligned}\mathrm{PL}\,(k,\omega)\propto|C_k|^2\,\mathrm{Re}\Big\{&\frac{in_{1k}\,(\overline{u}_{11}\overline{u}_{22}+\overline{u}_{31}\overline{u}_{42})}{\hbar\omega-E_1}+\frac{i\,(n_{1k}+1)\,(\overline{u}_{12}\overline{u}_{21}+\overline{u}_{32}\overline{u}_{41})}{\hbar\omega+E_1^*}+\frac{in_{2k}\,(\overline{u}_{13}\overline{u}_{24}+\overline{u}_{33}\overline{u}_{44})}{\hbar\omega-E_2}\\&+\frac{i\,(n_{2k}+1)\,(\overline{u}_{14}\overline{u}_{23}+\overline{u}_{34}\overline{u}_{43})}{\hbar\omega+E_2^*}\Big\},\end{aligned} \tag{23}$$

where C_k is called the Hopfield coefficient for the photonic component of the polaritons, and n_{1k} (n_{2k}) is the thermal population of quasiparticles associated with the density mode (spin mode). Different from the PL spectrum of a one-component poariton condensate, Equation (23) involves contributions from both the density- and spin-mode: the first (last) two terms correspond to the density (spin) mode, with the negative branch contained in the second (fourth) term, respectively. In Fig. 3, we present the PL spectrum of a spinor polariton condensate for various parameters.

Let us first compare the PL spectrum in the unpolarized phase and polarized phase, respectively, considering for example the parameter regime $\gamma_R \ll \gamma_C$ and high temperature (larger than the relevant energy gap). As illustrated in Figs. 3(a1) and (c1), both plots show the positive and negative branches of the dispersions, due to large populations at high temperatures. Yet, a prominent feature of Fig. 3(c1) for the polarized phase, as compared to Fig. 3(a1) for the unpolarized phase, is the appearance of two separated sectors of dispersions, both in the positive and negative branches. This second dispersion sector, with a very narrow linewidth, corresponds to the spin mode which is weakly damped in the polarized phase. Instead, the dispersion of the spin mode does not appear in the unpolarized phase [see Fig. 3(a1)], as the spin mode there only has real energy and is undamped [see Fig. 1(b)]. Thus for the unpolarized phase in the present setup, only the density sector of dispersions are revealed by PL spectrum, see Fig. 3(a) and (b) for various parameters. As illustrated in Fig. 3(c2), at low temperatures, only the negative energy ghost branch of the spin mode becomes visible, due to strongly suppressed thermal population of the gapped positive-energy spin mode. In contrast, the spin-sector cannot be distinguished in Fig. 3(c3) corresponding to a fast reservoir regime, which can be attributed to the fact that, for this particular parameter choice, the real part of the spectra of the density mode is very close to the spin mode [see Fig. 2(a2)]. To conclude, the negative energy ghost branch of the spin mode can be clearly distinguished from that of the density mode in the PL spectra of a spinor polariton condensate in the polarized phase, where the spin mode is weakly damped. Its resolution is optimal when the (real part) energy of the spin mode is sufficiently separated from the density mode, such that it is still resolvable after taking into account of the finite linewidth of the spectrum of the density mode.

Turning back to the unpolarized phase, as discussed above, here only dispersions of the density mode can be visualized in the PL spectrum. In general, the width of the spectrum exhibits a significant broadening for $\gamma_R \ll \gamma_C$ [see e.g. Fig. 3(a1)] reflecting a strong damping of the density mode [see also Fig. 1(b3)]. Instead, a much narrower spectrum is shown in the fast reservoir limit [see Fig. 3(a3)], where the density mode only weakly decays. Notice that in Fig. 3(a3), despite high temperature, no fingerprints of the negative energy dispersion of density mode is observed. This is due to the fact that the corresponding Bogoliubov coefficients in Eq. (23) nearly vanishes for this specific parameter choices. Considering experimental relevant parameters, we plot the corresponding PL spectrum in the unpolarized phase in Fig. 3(b). Compared to Figs. 3(a), we see that the sign of g_{12}, does not qualitatively change the features of the PL spectrum in the unpolarized phase.

IV. CONCLUSION

To summarize, we have investigated the steady phases and the elementary excitations of a spinor polariton condensate within the mean-field description. We have identified two phases for a steady homogeneous spinor polariton condensate state, namely the unpolarized phase and the polarized phase. At the critical point, the spin density response function diverges and the energy gap of the spin mode closes. In addition, we have shown that the gapped spin modes are long lived in both phases and are robust to reservoir effects. The energy spectrum

of the density modes, by contrast, are strongly tailored by the reservoir polaritons, exhibiting qualitatively different behavior depending on reservoir parameters, such as becoming gapped in the slow reservoir limit as a result of the strong coupling between the dynamics of density and reservoir modulations. In addition, we have demonstrated that the energy dispersions presented in this work can be directly observed in the PL emission. In particular, we show that the negative energy ghost branch of the dispersion of the spin mode can be clearly visualized in the polarized phase, exhibiting a very narrow linewidth and distinguishable from that of density mode. That the spin mode is undamped in the unpolarized phase, leading to its absence in the corresponding PL spectrum, may be related to the fact that in our setup [see Eq. (3)], the density of the reservoir polaritons are assumed to be coupled to the total density - rather than the spin density - of the spinor polariton condensate. Hence an interesting subject of investigation in the future consists of cases with asymmetric couplings to reservoir polaritons or asymmetric decay rates of condensate polaritons.

ACKNOWLEDGMENTS

We thank Yan Xue, Chao Gao, and Biao Wu for stimulating discussions. This is supported by the NSFC of China (Grant Nos. 11274315 and 11374125) and Youth Innovation Promotion Association CAS (Grant No. 2013125). Y. H. acknowledges support from Changjiang Scholars and Innovative Research Team in University of Ministry of Education of China and PCSIRT (No. IRT13076) the NSFC of China (Grant No. 11434007). Z. D. Z. is supported by the NSFC of China (Grant No. 51331006).

* The corresponding author: zhxliang@gmail.com

[1] Hui Deng, Hartmut Haug, and Yoshihisa Yamamoto, "Exciton-polariton bose-einstein condensation," Rev. Mod. Phys. **82**, 1489–1537 (2010).
[2] Iacopo Carusotto and Cristiano Ciuti, "Quantum fluids of light," Rev. Mod. Phys. **85**, 299–366 (2013).
[3] T. Byrnes, N. Y. Kim, and Y. Yamamoto, "Exciton-polariton condensates," Nat. Phys. **10**, 803–813 (2014).
[4] J. Kasprzak, M. Richard, S. Kundermann, A. Baas, P. Jeambrun, J. M. J. Keeling, F. M. Marchetti, M. H. Szymanska, R. Andre, J. L. Staehli, V. Savona, P. B. Littlewood, B. Deveaud, and Le Si Dang, "Bose-einstein condensation of exciton polaritons," Nature **443**, 409–414 (2006).
[5] R. Balili, V. Hartwell, D. Snoke, L. Pfeiffer, and K. West, "Bose-einstein condensation of microcavity polaritons in a trap," Science **316**, 1007–1010 (2007).
[6] Hui Deng, Gregor Weihs, Charles Santori, Jacqueline Bloch, and Yoshihisa Yamamoto, "Condensation of semiconductor microcavity exciton polaritons," Science **298**, 199–202 (2002).
[7] Yongbao Sun, Patrick Wen, Yoseob Yoon, Gangqiang Liu, Mark Steger, Loren N. Pfeiffer, Ken West, David W. Snoke, and Keith A. Nelson, "Bose-einstein condensation of long-lifetime polaritons in thermal equilibrium," Phys. Rev. Lett. **118**, 016602 (2017).
[8] Michiel Wouters and Iacopo Carusotto, "Excitations in a nonequilibrium bose-einstein condensate of exciton polaritons," Phys. Rev. Lett. **99**, 140402 (2007).
[9] M. H. Szymańska, J. Keeling, and P. B. Littlewood, "Nonequilibrium quantum condensation in an incoherently pumped dissipative system," Phys. Rev. Lett. **96**, 230602 (2006).
[10] Tim Byrnes, Tomoyuki Horikiri, Natsuko Ishida, Michael Fraser, and Yoshihisa Yamamoto, "Negative bogoliubov dispersion in exciton-polariton condensates," Phys. Rev. B **85**, 075130 (2012).
[11] Yan Xue and Michał Matuszewski, "Creation and abrupt decay of a quasistationary dark soliton in a polariton condensate," Phys. Rev. Lett. **112**, 216401 (2014).
[12] G. Dagvadorj, J. M. Fellows, S. Matyjaśkiewicz, F. M. Marchetti, I. Carusotto, and M. H. Szymańska, "Nonequilibrium phase transition in a two-dimensional driven open quantum system," Phys. Rev. X **5**, 041028 (2015).
[13] Torsten Karzig, Charles-Edouard Bardyn, Netanel H. Lindner, and Gil Refael, "Topological polaritons," Phys. Rev. X **5**, 031001 (2015).
[14] Vladimir N. Gladilin and Michiel Wouters, "Normal and superfluid fractions of inhomogeneous nonequilibrium quantum fluids," Phys. Rev. B **93**, 134511 (2016).
[15] Jamir Marino and Sebastian Diehl, "Driven markovian quantum criticality," Phys. Rev. Lett. **116**, 070407 (2016).
[16] Matteo Biondi, Evert P. L. van Nieuwenburg, Gianni Blatter, Sebastian D. Huber, and Sebastian Schmidt, "Incompressible polaritons in a flat band," Phys. Rev. Lett. **115**, 143601 (2015).
[17] A. V. Nalitov, D. D. Solnyshkov, and G. Malpuech, "Polariton $\mathbb{Z}$ topological insulator," Phys. Rev. Lett. **114**, 116401 (2015).
[18] Liang He, Lukas M. Sieberer, and Sebastian Diehl, "Space-time vortex driven crossover and vortex turbulence phase transition in one-dimensional driven open condensates," Phys. Rev. Lett. **118**, 085301 (2017).
[19] H. Ohadi, A. Dreismann, Y. G. Rubo, F. Pinsker, Y. del Valle-Inclan Redondo, S. I. Tsintzos, Z. Hatzopoulos, P. G. Savvidis, and J. J. Baumberg, "Spontaneous spin bifurcations and ferromagnetic phase transitions in a spinor exciton-polariton condensate," Phys. Rev. X **5**, 031002 (2015).
[20] A. Askitopoulos, K. Kalinin, T. C. H. Liew, P. Cilibrizzi, Z. Hatzopoulos, P. G. Savvidis, N. G. Berloff, and P. G. Lagoudakis, "Nonresonant optical control of a spinor polariton condensate," Phys. Rev. B **93**, 205307 (2016).
[21] T. K. Paraiso, Michiel Wouters, Y. Leger, F. Morier-genoud, and Benoit Deveaudpledran, "Multistability of a coherent spin ensemble in a semiconductor microcavity," Nat. Mater. **9**, 655–660 (2010).

[22] S. S. Gavrilov, A. V. Sekretenko, S. I. Novikov, C. Schneider, Sven Hofling, M. Kamp, A. Forchel, and V. D. Kulakovskii, "Polariton multistability and fast linear-to-circular polarization conversion in planar microcavities with lowered symmetry," Appl. Phys. Lett. **102**, 011104 (2013).

[23] P. G. Lagoudakis, P. G. Savvidis, J. J. Baumberg, D. M. Whittaker, P. R. Eastham, M. S. Skolnick, and J. S. Roberts, "Stimulated spin dynamics of polaritons in semiconductor microcavities," Phys. Rev. B **65**, 161310 (2002).

[24] A. Kavokin, P. G. Lagoudakis, G. Malpuech, and J. J. Baumberg, "Polarization rotation in parametric scattering of polaritons in semiconductor microcavities," Phys. Rev. B **67**, 195321 (2003).

[25] T. Gao, P. S. Eldridge, T. C. H. Liew, S. I. Tsintzos, G. Stavrinidis, G. Deligeorgis, Z. Hatzopoulos, and P. G. Savvidis, "Polariton condensate transistor switch," Phys. Rev. B **85**, 235102 (2012).

[26] D. Ballarini, M. De Giorgi, E. Cancellieri, R. Houdré, E. Giacobino, R. Cingolani, A. Bramati, G. Gigli, and D. Sanvitto, "Corrigendum: All-optical polariton transistor," Nat. Commun. **5**, 5625 (2014).

[27] Lev A. Smirnov, Daria A. Smirnova, Elena A. Ostrovskaya, and Yuri S. Kivshar, "Dynamics and stability of dark solitons in exciton-polariton condensates," Phys. Rev. B **89**, 235310 (2014).

[28] A. Amo, T. C. H. Liew, C. Adrados, R. Houdré, E. Giacobino, A. V. Kavokin, and A. Bramati, "Exciton-polariton spin switches," Nat. Photon. **4**, 361–366 (2010).

[29] E. Kammann, T. C. H. Liew, H. Ohadi, P. Cilibrizzi, P. Tsotsis, Z. Hatzopoulos, P. G. Savvidis, A. V. Kavokin, and P. G. Lagoudakis, "Nonlinear optical spin hall effect and long-range spin transport in polariton lasers," Phys. Rev. Lett. **109**, 036404 (2012).

[30] T. Espinosa-Ortega and T. C. H. Liew, "Complete architecture of integrated photonic circuits based on and and not logic gates of exciton polaritons in semiconductor microcavities," Phys. Rev. B **87**, 195305 (2013).

[31] Pallab Bhattacharya, Bo Xiao, Ayan Das, Sishir Bhowmick, and Junseok Heo, "Solid state electrically injected exciton-polariton laser," Phys. Rev. Lett. **110**, 206403 (2013).

[32] C. Schneider, A. Rahimi-Iman, N. Y. Kim, J. Fischer, I. G. Savenko, M. Amthor, M. Lermer, A. Wolf, L. Worschech, V. D. Kulakovskii, I. A. Shelykh, M. Kamp, S. Reitzenstein, A. Forchel, Y. Yamamoto, and S. Höfling, "An electrically pumped polariton laser," Nature **497**, 348–352 (2013).

[33] C. Antón, S. Morina, T. Gao, P. S. Eldridge, T. C. H. Liew, M. D. Martín, Z. Hatzopoulos, P. G. Savvidis, I. A. Shelykh, and L. Viña, "Optical control of spin textures in quasi-one-dimensional polariton condensates," Phys. Rev. B **91**, 075305 (2015).

[34] F. Pinsker and H. Flayac, "On-demand dark soliton train manipulation in a spinor polariton condensate," Phys. Rev. Lett. **112**, 140405 (2014).

[35] C. Sturm, D. Solnyshkov, O. Krebs, A. Lemaître, I. Sagnes, E. Galopin, A. Amo, G. Malpuech, and J. Bloch, "Nonequilibrium polariton condensate in a magnetic field," Phys. Rev. B **91**, 155130 (2015).

[36] T. C. H. Liew, O. A. Egorov, M. Matuszewski, O. Kyrienko, X. Ma, and E. A. Ostrovskaya, "Instability-induced formation and nonequilibrium dynamics of phase defects in polariton condensates," Phys. Rev. B **91**, 085413 (2015).

[37] N. Takemura, S. Trebaol, M. Wouters, M. T. Portella-Oberli, and B. Deveaud, "Polaritonic feshbach resonance," Nat. Phys. **10**, 500–504 (2014).

[38] A. A. Elistratov and Yu. E. Lozovik, "Coupled exciton-photon bose condensate in path integral formalism," Phys. Rev. B **93**, 104530 (2016).

[39] K. Dunnett and M. H. Szymańska, "Keldysh field theory for nonequilibrium condensation in a parametrically pumped polariton system," Phys. Rev. B **93**, 195306 (2016).

[40] Michael Buchhold, Benjamin Everest, Matteo Marcuzzi, Igor Lesanovsky, and Sebastian Diehl, "Nonequilibrium effective field theory for absorbing state phase transitions in driven open quantum spin systems," Phys. Rev. B **95**, 014308 (2017).

[41] Ehud Altman, Lukas M. Sieberer, Leiming Chen, Sebastian Diehl, and John Toner, "Two-dimensional superfluidity of exciton polaritons requires strong anisotropy," Phys. Rev. X **5**, 011017 (2015).

[42] Tom Bienaimé, Eleonora Fava, Giacomo Colzi, Carmelo Mordini, Simone Serafini, Chunlei Qu, Sandro Stringari, Giacomo Lamporesi, and Gabriele Ferrari, "Spin-dipole oscillation and polarizability of a binary bose-einstein condensate near the miscible-immiscible phase transition," Phys. Rev. A **94**, 063652 (2016).

[43] Marta Abad and Alessio Recati, "A study of coherently coupled two-component bose-einstein condensates," Eur. Phys. J. D **67**, 1–11 (2013).

[44] Z. X. Liang, Xi Dong, Z. D. Zhang, and Biao Wu, "Sound speed of a bose-einstein condensate in an optical lattice," Phys. Rev. A **78**, 023622 (2008).

[45] Wu Li, Lei Chen, Zhu Chen, Ying Hu, Zhidong Zhang, and Zhaoxin Liang, "Probing the flat band of optically trapped spin-orbital-coupled bose gases using bragg spectroscopy," Phys. Rev. A **91**, 023629 (2015).

[46] Zhu Chen and Zhaoxin Liang, "Ground-state phase diagram of a spin-orbit-coupled bosonic superfluid in an optical lattice," Phys. Rev. A **93**, 013601 (2016).

[47] André Eckardt, Christoph Weiss, and Martin Holthaus, "Ground-state energy and depletions for a dilute binary bose gas," Phys. Rev. A **70**, 043615 (2004).

[48] Kerwyn Casey Huang, Peter Bienstman, John. D. Joannopoulos, Keith A. Nelson, and Shanhui Fan, "Phonon-polariton excitations in photonic crystals," Phys. Rev. B **68**, 075209 (2003).

[49] Jian Wang, Wei Xie, Long Zhang, Dan Xu, Wenhui Liu, Jian Lu, Yinglei Wang, Jie Gu, Yan Chen, Xuechu Shen, and Zhanghai Chen, "Exciton-polariton condensate induced by evaporative cooling in a three-dimensionally confined microcavity," Phys. Rev. B **91**, 165423 (2015).

[50] S. Utsunomiya, L. Tian, G. Roumpos, C. W. Lai, N. Kumada, T. Fujisawa, M. Kuwata-Gonokami, A. Loffler, S. Höfling, A. Forchel, and Y. Yamamoto, "Observation of bogoliubov excitations in exciton-polariton condensates," Nat. Phys. **4**, 700–705 (2008).

[51] Marc Aβmann, Jean-Sebastian Tempel, Franziska Veit, Manfred Bayer, Arash Rahimi-Iman, Andreas Löffler, Sven Höfling, Stephan Reitzenstein, Lukas Worschech, and Alfred Forchel, "From polariton condensates to highly photonic quantum degenerate states of bosonic matter," Proc. Natl. Acad. Sci. U.S.A. **108**, 1804–1809 (2011).

[52] V. Kohnle, Y. Léger, M. Wouters, M. Richard, M. T. Portella-Oberli, and B. Deveaud-Plédran, "From single particle to superfluid excitations in a dissipative polariton

gas," Phys. Rev. Lett. **106**, 255302 (2011).
[53] Maciej Pieczarka, Marcin Syperek, Łukasz Dusanowski, Jan Misiewicz, Fabian Langer, Alfred Forchel, Martin Kamp, Christian Schneider, Sven Höfling, Alexey Kavokin, and Grzegorz Sęk, "Ghost branch photoluminescence from a polariton fluid under nonresonant excitation," Phys. Rev. Lett. **115**, 186401 (2015).
[54] Cristiano Ciuti, Paolo Schwendimann, and Antonio Quattropani, "Parametric luminescence of microcavity polaritons," Phys. Rev. B **63**, 041303 (2001).